Determination of reduced scattering coefficient of biological tissue from a needle-like probe

Maureen Johns
Department of Bioengineering, University of Texas at Arlington, Arlington, TX 76019
Moejohns@aol.com

Cole A. Giller
Department of Neurological Surgery, University of Texas Southwestern Medical Center at Dallas, Dallas, TX 75390
Cole.Giller@UTSouthwestern.edu

Dwight C. German
Department of Psychiatry, University of Texas Southwestern Medical Center at Dallas, Dallas, TX 75390
Dwight.German@UTSouthwestern.edu

Hanli Liu
Department of Bioengineering, University of Texas at Arlington, Arlington, TX 76019
Hanli@uta.edu

Abstract: Detection of interactions between light and tissue can be used to characterize the optical properties of the tissue. The purpose of this paper is to develop an algorithm that determines the reduced scattering coefficient (μ_s') of tissues from a single optical reflectance spectrum measured with a small source-detector separation. A qualitative relationship between μ_s' and optical reflectance was developed using both Monte Carlo simulations and empirical tissue calibrations for each of two fiber optic probes with 400-μm and 100-μm fibers. Optical reflectance measurements, using a standard frequency-domain oximeter, were performed to validate the calculated μ_s' values. The algorithm was useful for determining μ_s' values of *in vivo* human fingers and rat brain tissues.

OCIS codes: (170.3660) Light propagation in tissues; (170.4580) Optical diagnostics for medicine; (170.6510) Spectroscopy, tissue diagnostics; (290.4210) Multiple scattering.

References and Links

1. H.R. Eggert and V. Blazek, "Optical Properties of Human Brain Tissue, Meninges, and Brain Tumors in the Spectral Range of 200 to 900 nm," Neurosurg. **21**, 459-464 (1987).
2. M. Johns, C.A. Giller and H. Liu, "Computational and *In Vivo* Investigation of Optical Reflectance from Human Brain to Assist Neurosurgery," J. Biomed. Opt. **3**, 437-445 (1998).
3. G. Zonios, L.T. Perelman, V. Backman, R. Manoharan, M. Fitzmaurice, J. Van Dam and M.S. Feld, "Diffuse Reflectance Spectroscopy of Human Adenomatous Colon Polyps In Vivo," Appl. Opt. **38**, 6628-6637 (1999).
4. J.R. Mourant, I.J. Bigio, J. Boyer, T.M. Johnson, J. Lacey, A.G. Bohorhoush and M. Mellow, "Elastic Scattering Spectroscopy as a Diagnostic Tool for Differentiating Pathologies in the Gastrointestinal Tract: Preliminary Testing," J. Biomed. Opt. **1**, 192-199 (1996).
5. A.M.K. Nilsson, C. Sturesson, D.L. Liu and S. Andersson-Engels, "Changes in spectral shape of tissue optical properties in conjunction with laser-induced thermotherapy," Appl. Opt. **37**, 1256-1267 (1998).
6. J.S. Dam, T. Dalgaard, P.E. Fabricius and S. Andersson-Engels, "Multiple polynomial regression method for determination of biomedical optical properties from integrating sphere measurements," Appl. Opt. **39**, 1202-1209 (2000).
7. A.M.K. Nilsson, R. Berg and S. Andersson-Engels, "Measurements of the optical properties of tissue in conjunction with photodynamic therapy," Appl. Opt. **34**, 4609-4619 (1995).
8. S.-P. Lin, L. Wang, S.L. Jacques, and F.K. Tittel, "Measurement of tissue optical properties by the use of oblique-incidence optical fiber reflectometry," Appl. Opt. **36**, 136-143 (1997).

#7239 - $15.00 USD Received 22 April 2005; revised 7 June 2005; accepted 9 June 2005

9. F.Bevilacqua, D.Piguet,P. marguet, J.D. Gross, B.J. Tromberg, and C. Depeursinge, "In vivo local determination of tissue optical properties : applications to human brain," Appl. Opt. **38**, 4939-4950 (1999).
10. A. Amelink, A.P. van den Heuvel, W.J. de Wolf, D.J. Robinson, and H.J. Sterenborg, "Monitoring PDT by means of superficial reflectance spectroscopy,"J. Photochem. Photobiol. B **79**, 243-251 (2005).
11. C.A. Giller, H. Liu**,** P. P. Gurnani, S. Victor, U. Yazdani, and D. C. German, "Validation of a Near-Infrared Probe for Detection of Thin Intracranial White Matter Structures," J. Neurosurg. **98**, 1299-1306 (2003).
12. C.A. Giller, M. Johns and H. Liu, "Use of an intracranial near-infrared probe for localization during stereotactic surgery for movement disorders," J. Neurosurg. **93**, 498-505 (2000).
13. F. Bevilacqua and C. Depeursinge, "Monte Carlo study of diffuse reflectance at source-detector separations close to one transport mean free path," J. Opt. Soc. Am. **16**, 2935-2945 (1999).
14. J. S. Dam, C. B. Pedersen, T Dalgaard, P. E. Fabricius, P. Aruna, and S. Andersson-Engels, "Fiber-optic probe for noninvasive real-time determination of tissue optical properties at multiple wavelengths," Appl. Opt. **40**, 1155-1164 (2001).
15. L.H. Wang, S.L. Jacques, and L-Q Zheng, "MCML-Monte Carlo modeling of photon transport in multi-layered tissues," Comp. Meth. Prog. Biomed. **47**, 131-146 (1995).
16. L.H. Wang, S.L. Jacques, and L-Q Zheng, "CONV-Convolution for responses to a finite diameter photon beam incident on multi-layered tissues," Comp. Meth. Prog. Biomed. **54**, 141-150 (1997).
17. http://oilab.tamu.edu/mc.html
18. A. Kienle, L. Lilge, M.S. Patterson, R. HIbst, R. Steiner and B.C. Wilson, "Spatially resolved absolute diffuse reflectance measurements for noninvasive determination of the optical scattering and absorption coefficients of biological tissue," Appl. Opt. **35**, 2304-2314 (1996).
19. F.A. Duck, *Physical Properties of Tissue: A Comprehensive Reference Book* (Academic Press, San Diego, 1990), p.62.
20. W-F Cheong, S.A. Prahl and A.J. Welch, "A Review of the Optical Properties of Biological Tissues," IEEE J. of Quan. Elec. **26**, 2166-2185 (1990).
21. P. van der Zee, M. Essenpreis, and D.T. Delpy, "Optical properties of brain tissue," Proc. SPIE **1888**, 454-465, (1993).
22. P. Gurnani, "Near Infrared Spectroscopic Measurement of Human and Animal Brain Structures," Master Thesis, The University of Texas at Arlington, Arlington, TX, May, 2003.
23. http://www.iss.com/Products/oxiplex.html
24. Z. Qian, S. Victor, Y. Gu, C.A. Giller, and H. Liu, " 'Look-Ahead Distance' of a fiber probe used to assist neurosurgery: phantom and Monte Carlo study," Opt. Express **11** 1844-1855, (2003).
25. M. Johns, C.A. Giller, and H. Liu, "Determination of hemoglobin saturation in blood-perfused tissues using reflectance spectroscopy with small source-detector separations," Appl. Spectrosc. **55**, 1686-1694 (2001).
26. M. Solonenko, R. Cheung, T.M. Busch, A. Kachur, G.M. Griffin, T. Vulcan, T.C. Zhu, H.W. Wang, S.M. Hahn, and A.G. Yodh, "In vivo reflectance measurement of optical properties, blood oxygenation and motexafin lutetium uptake in canine large bowels, kidneys and prostates," Phys. Med. Biol. **47**, 857-73 (2002).
27. G. Paxinos and C. Watson, "The rat brain in stereotaxic coordinates," Academic Press Inc., 4th edition, London, (1998).
28. M. Johns, "Optical properties of living tissues determined in vivo using a thin fiber optic probe," Ph.D. Dissertation, The University of Texas at Arlington, Arlington, TX, December, (2003).
29. A.E. Cerussi, A.J. Berger, F. Bevilacqua, N. Shah, D. Jakubowski, J. Bulter, R.F. Holcombe and B.J. Tromberg, "Sources of Absorption and Scattering Contrast for Near-Infrared Optical Mammography," Acad Radiol. **8**, 211-218 (2001).
30. T. Durduran, R. Choe, J.P. Culver, L. Zubkov, M.J. Holboke, J. Giammarco, B. Chance and A.G. Yodh, "Bulk optical properties of healthy female breast tissue," Phys. Med. Biol. **47**, 2847-2861 (2002).
31. H. Eggert, V. Blazek, "Optical properties of human brain tissue, meninges, and brain tumors in the spectral range of 200 to 900 nm," Neurosurgery **21**, 459-464, (1987).
32. H. Schwarzmaier, A. Yaroslavsky, I. Yaroslavsky, G. Thomas, K. Thomas, U. Frank, P. Schulze, R. Schober, "Optical properties of native and coagulated human brain structures," Proc. SPIE **2970**, 492-499 (1997).
33. H. Shangguan, S.A. Prahl, S.L. Jacques and L.W. Casperson, "Pressure effects on soft tissues monitored by changes in tissue optical properties," in *Laser-Tissue Interaction IX*, S.L. Jacques Ed., Proc. SPIE **3254**, 366-371 (1998).

1. Introduction

In recent years, optical reflectance spectroscopy has been used to extract physiological information from human tissues [1-3] and organs [4]. The fiber optic methods provide a low risk, low cost, and minimally invasive way to investigate characteristics of human tissues and structures. Numerous studies have shown that the reduced scattering coefficient (μ_s') can be obtained using an integrating sphere in combination with a curve-fitting procedure between experimental data and Monte Carlo simulations [5-7]. While this technique is effective, it

#7239 - $15.00 USD Received 22 April 2005; revised 7 June 2005; accepted 9 June 2005

requires *ex vivo* tissues for the integrating sphere and increases computational time due to complex curve fitting. In *ex vivo* measurements, it is uncertain whether the optical properties of tissues are significantly affected by such factors as 1) lack of blood perfusion after excision, 2) length of time between excision and measurement, 3) the use of saline for re-hydration purposes, and 4) placement of the sample between two pieces of glass. Thus, direct *in vivo* measurements of light scattering from living tissues are desirable but impossible with the integrating sphere approach. It is highly desirable to develop an algorithm with the ability to quantify the optical scattering property based on optical reflectance measured from *in vivo* tissues in real time. In recent years, researchers have made significant efforts in developing methods to measure the optical properties of tissue *in vivo* [3, 5, 8-10].

In recent studies, we have developed a needle-like, near infrared (NIR) probe with a small source-detector separation (100-400 μm) to identify gray and white matter structures in the living human and animal brain [2, 11, 12]. The NIR probes had an outer diameter of 1.3 mm used in the human study [11] and of 0.45 mm for the animal study [12]. Both kinds of probes contained two 100-μm fibers to deliver light to and collect light from the brain tissue. We have shown that the optical reflectance spectra exhibited significant differences between gray and white matter structures [2, 11, 12]. The goal of the present paper is to develop an algorithm that allows us to extract the light scattering properties (μ_s') of brain tissues *in vivo* from a single reflectance measurement with a needle-like probe. This is accomplished by developing a qualitative relationship between μ_s' and optical reflectance using both Monte Carlo simulations and empirical calibrations. Then, the developed algorithm is further validated using a standard frequency-domain oximeter and applied for determining μ_s' values of *in vivo* human fingers and rat brain tissues.

2. Monte Carlo simulations

With the definition of optical reflectance being the number of photons per unit area that are reflected back from a measured sample, a single, optical reflectance spectrum contains a large amount of information about the reflecting medium. Currently, few publications have presented an analytical expression that directly associates μ_s' with the reflectance measurements [13, 14]. In our study, to develop such a relationship, we utilized a well tested [15, 16] and publicly available [17] Monte Carlo simulation software to simulate actual reflectance measurements in tissues at an appropriate source-detector separation with a set of input parameters. Such parameters include $g = 0.9$ and $n = 1.38$ [18, 19], where g is scattering anisotropy, and n is the index of refraction. In common with our previous work [2], we used an infinitely large slab with only one bulk layer, and the tissue layer thickness (d) was chosen to be 10 cm. The simulations were performed with a spatial step size of 0.05 mm (or 50 μm) and a maximum detection radius of 1.5 mm (or 1500 μm). During the simulations, μ_s' was varied from 1-60 cm^{-1} for each of the four absorption coefficients: $\mu_a = 0.01$, 0.1, 0.25 and 0.5 cm^{-1}. These absorption and scattering values were selected based on the values that may be commonly found in tissues [20, 21]. The Monte Carlo output results were used to develop a relationship between the simulated optical reflectance and μ_s' for each of the four absorption coefficients. Since the output of Monte Carlo simulations for reflectance depends on the product of μ_s and $(1-g)$, rather than their individual values [15, 16, 22], a fixed value of $g = 0.9$ in the simulation still permits us to simulate a broad range of tissue scattering properties by combining different g and μ_s values.

Figure 1 shown below plots four sets of simulated reflectance (R_{sim}) versus μ_s' at $\mu_a = 0.01$, 0.1, 0.25, 0.5 cm^{-1}, with a source-detector separation of 400 μm. This separation matches the actual fiber separation in one of our needle probes used in the *in vivo* and *in vitro* experiments, and this probe is referred to as the 400-μm probe throughout the paper. On close inspection of this figure, we see that the reflectance values seem a little lower for higher values of absorption, as expected.

#7239 - $15.00 USD Received 22 April 2005; revised 7 June 2005; accepted 9 June 2005

In general, a student t-test is a fundamental statistical process to compare the two means of two groups of data. Normally, if p is less than 0.05 ($p < 0.05$), the two means of the two groups are significantly different; if $p > 0.05$, the two means have no significant differences. After such statistical analysis, we learned that the differences among the reflectance with μ_a values from 0.01 cm^{-1} to 0.5 cm^{-1} are insignificant ($p>0.8$). This permits us to pool all the data together and to obtain a linear relationship between the simulated reflectance, R_{sim}, and μ_s' as

$$R_{sim}(\lambda_0) = 0.404\ \mu_s'(\lambda_0) + 0.582. \qquad (1)$$

Specifically, the four sets of data were averaged at each μ_s' value, and the mean values of reflectance were used to generate Eq. (1), with a correlation coefficient of R=0.99. It is known that the μ_s' values of biological tissues are weakly wavelength dependent, and this dependence is sufficiently weak over the near infrared (NIR) range. Thus, we may use Eq. (1) for wavelength values (λ_0) within 650 nm to 900 nm. Notice that a simple linear fitting is a desirable starting approach, while the data given in Fig. 1 may be fitted well with a 2nd order polynomial equation. Error analysis by the end of the algorithm development will justify if the linear approach is reasonable, or a higher order approach is needed.

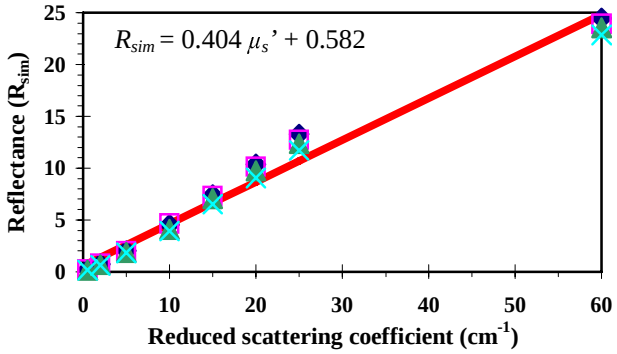

Fig. 1. Simulated relationship between reflectance and the reduced scattering coefficient at varying μ_a values of 0.01 cm^{-1} (solid diamond), 0.1 cm^{-1} (open square), 0.25 cm^{-1} (solid triangle), and 0.5 cm^{-1} (cross), with the source-detector separation fixed at 400 microns. The unit for reflectance is the number of photons /cm^2.

To associate the simulated reflectance, $R_{sim}(\lambda_0)$, and the measured reflectance, $R_m(\lambda_0)$, we assumed a simple proportion between them as

$$R_{m\text{-}400}(\lambda_0) = a_{0\text{-}400}\, R_{sim\text{-}400}(\lambda_0) = a_{0\text{-}400}\ [0.404\ \mu_s'(\lambda_0) + 0.582], \qquad (2)$$

where $a_{0\text{-}400}$ is an overall intensity factor for the 400-μm probe. The a_0 factor is used to relate μ_s' values and the measured R_m values, as shown in Eq. (2). The experimental set-up, fiber geometry, and the diameter of the internal fibers each contribute to the a_0 term. While Monte Carlo simulations do provide a reasonable estimate of light behavior through a turbid medium, they cannot account for all influences from the various system components that contribute to the actual measured signal. Therefore, the a_0 term is determined using an empirical calibration method that is to be described in Section 3.

An optical needle probe with a source-detector separation of 100 μm was also used for both *in vivo* and *in vitro* measurements. A similar Monte Carlo simulation was performed to obtain the relationship between $R_{sim}(\lambda_0)$ and $\mu_s'(\lambda_0)$ for the 100 μm probe, which will be referred to as the 100-μm probe throughout the paper. Using the similar methodology to that given above, the simulated data with four different μ_a values were averaged at each μ_s' value

#7239 - $15.00 USD Received 22 April 2005; revised 7 June 2005; accepted 9 June 2005

for the 100-μm probe (figure not shown), and a linear relationship between $R_{m\text{-}100}(\lambda_0)$ and $\mu_s'(\lambda_0)$ is obtained as follows:

$$R_{m\text{-}100}(\lambda_0) = a_{0\text{-}100}\, R_{sim\text{-}100}(\lambda_0) = a_{0\text{-}100}\ [1.670\ \mu_s'(\lambda_0) - 1.544]. \quad (3)$$

With a chosen probe (either the 400-μm or the 100-μm), quantification of a_0 becomes the key issue for final determination of μ_s' from the measured R_m, as seen in Eqs. (2) and (3). An experimental approach was taken to empirically quantify a_0 for each of the two probes.

3. Algorithms to determine a_0 and μ_s'

Measurements of μ_s' were obtained from a diluted solution of Intralipid (20% Intralipid, Pharmacia and Up-John, Clayton, NC) using a dual-channel, frequency-domain oximeter (ISS, Champaign, IL) [23], which will be described more in Section 4.1. Simultaneously, the 400-micron fiber optic probe was used with a portable CCD spectrometer (SD2000, Ocean Optics, FL) to obtain the reflectance at two selected wavelengths, 750 nm and 830 nm. The Intralipid solution was serially diluted to include Intralipid concentrations between 0.5% and 8% to cover a broad range of light scattering properties. Additional details for the experimental setup are given in Section 4.

3.1 Algorithms to determine a_0 and μ_s' for the 400-μm probe

Using Eq. (2) to solve for $a_{0\text{-}400}$, we obtain

$$a_{0-400} = \frac{R_{m-400}(\lambda_0)}{0.404 * \mu_s'(\lambda_0) + 0.5819}. \quad (4)$$

Based on the measured values of $R_{m\text{-}400}$ from the portable spectrometer and μ_s' from the ISS oximeter, individual $a_{0\text{-}400}$ values for each experiment can be obtained using equation (4). Figure 2(a) shows the relationship between the calculated $a_{0\text{-}400}$ values and corresponding measured $R_{m\text{-}400}$ obtained from 5 individual experiments at 750 nm and 830 nm. The 5 sets of data were pooled here for the Intralipid concentrations between 0.5 and 4%.

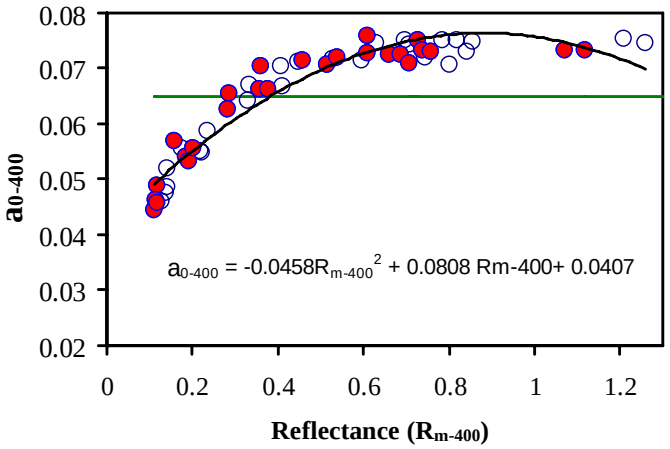

Fig. 2. (a). Overall intensity factor, $a_{0\text{-}400}$, versus measured reflectance, $R_{m\text{-}400}$, at 750 nm (open blue circles) and at 830 nm (filled red circles) for the 400-μm probe. An average $a_{0\text{-}400}$ value is shown as the solid green line while the solid black curve is a quadratic fit for the data.

Our statistical analysis for Fig. 2(a) shows that the mean $a_{0\text{-}400}$ value at 750 nm (0.066 ± 0.01) is not statistically different from the mean $a_{0\text{-}400}$ value at 830 nm (0.065 ± 0.01; $p > 0.5$). Thus, pooling the data from 750 nm and 830 nm allows the fitted equation to represent the

#7239 - $15.00 USD Received 22 April 2005; revised 7 June 2005; accepted 9 June 2005

data within the spectral range between 750 nm to 830 nm rather than fixed at a specific wavelength. Ideally, $a_{0\text{-}400}$ is expected to be constant and independent of $R_{m\text{-}400}$; however, Figure 2(a) shows that $a_{0\text{-}400}$ varies slightly with $R_{m\text{-}400}$. A quadratic fitting between $a_{0\text{-}400}$ and $R_{m\text{-}400}$ can be obtained in Eq. (5) with a correlation coefficient of R=0.96:

$$a_{0\text{-}400}(\lambda_0) = -0.0458\ R_{m\text{-}400}(\lambda_0)^2 + 0.0808\ R_{m\text{-}400}(\lambda_0) + 0.0407, \tag{5}$$

where λ_0 = 750 nm - 830 nm.

Figure 2(a) also shows a mean $a_{0\text{-}400}$ of 0.065 ± 0.01. This was calculated by taking a mean of all data points (at both 750 nm and 830 nm) given in Fig. 2(a). Detailed results will be given in Section 5 to compare the calculated μ_s' values using both the polynomial $a_{0\text{-}400}$ and the constant $a_{0\text{-}400}$ value.

Furthermore, substituting the constant $a_{0\text{-}400}$ or Eq. (5) into Eq. (2) and solving for μ_s' lead to empirically derived relationships between the μ_s' and the measured reflectance, $R_{m\text{-}400}$, for the 400-μm probe, as given below:

$$\mu_s'(\lambda_0) = \frac{R_{m-400}(\lambda_0) - 0.5819\ a_{0-400}(\lambda_0)}{0.404\ a_{0-400}(\lambda_0)}, \tag{6a}$$

$$\mu_s'(\lambda_0) = \frac{R_{m-400}(\lambda_0) - 0.5819\ [0.065]}{0.404\ [0.065]}, \tag{6b}$$

$$\mu_s'(\lambda_0) = \frac{R_{m-400}(\lambda_0) - 0.5819\left[-0.0458 R_{m-400}(\lambda_0)^2 + 0.0808 R_{m-400}(\lambda_0) + 0.0407\right]}{0.404\left[-0.0458 R_{m-400}(\lambda_0)^2 + 0.0808 R_{m-400}(\lambda_0) + 0.0407\right]}, \tag{6c}$$

where Eqs. (6b) and (6c) are for the constant $a_{0\text{-}400}$ and quadratic $a_{0\text{-}400}$, respectively.

3.2 Algorithms to determine a_0 and μ_s' for the 100-μm probe

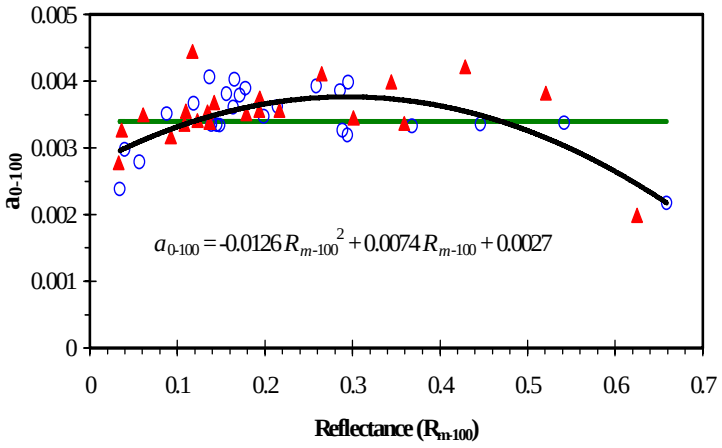

Fig. 2. (b). Overall intensity factor, $a_{0\text{-}100}$, versus measured reflectance, $R_{m\text{-}100}$, at 750 nm (open blue circles) and 830 nm (filled red triangles) for the 100-μm probe. An average $a_{0\text{-}400}$ value is shown as the solid green line, while the solid black curve is a quadratic fit for the data.

Similarly, an expression for $a_{0\text{-}100}$ was developed for the 100-μm probe. Figure 2(b) shows the relationship between the $a_{0\text{-}100}$ values and corresponding measured reflectance, $R_{m\text{-}}$

#7239 - $15.00 USD Received 22 April 2005; revised 7 June 2005; accepted 9 June 2005

$_{100}$, obtained from 8 individual experiments at 750 nm and 830 nm. The 8 sets of data were pooled, and the $a_{0\text{-}100}$ and reflectance values were averaged at each Intralipid concentration, ranging between 1-8% in this set of experiments. Statistical analysis shows that the mean $a_{0\text{-}100}$ value at 750 nm (0.0034 ± 0.0005) is not statistically different from the mean $a_{0\text{-}100}$ value at 830 nm (0.0034 ± 0.0006; $p > 0.1$).

A quadratic fitting between $a_{0\text{-}100}$ and $R_{m\text{-}100}$ can be also obtained in Eq. (7) for the 100-μm probe. Figure 2(b) shows a constant value of $a_{0\text{-}100}$, i.e., 0.0034 ± 0.0005, which was obtained by finding an average $a_{0\text{-}100}$ of all the data given in Figure 2(b). In Section 5, detailed comparison will demonstrate that the constant $a_{0\text{-}100}$ gives better μ_s' determination for the 100-μm probe.

$$a_{0\text{-}100}(\lambda_0) = -0.0126\ R_{m\text{-}100}(\lambda_0)^2 + 0.0074\ R_{m\text{-}100}(\lambda_0) + 0.0027. \quad (7)$$

Using the approach similar to that in obtaining Eq. (6), we substitute the constant $a_{0\text{-}100}$ and the quadratic $a_{0\text{-}100}$ (i.e., Eq. (7)) into Eq. (2), respectively, and solve for μ_s'. Then, we arrive at empirically derived relationships between μ_s' and $R_{m\text{-}100}$ for the 100-μm probe:

$$\mu_s'(\lambda_0) = \frac{R_{m-100}(\lambda_0) + 1.5437\ a_{0-100}(\lambda_0)}{1.6696\ a_{0-100}(\lambda_0)}, \quad (8a)$$

$$\mu_s'(\lambda_0) = \frac{R_{m-100}(\lambda_0) + 1.5437\ [0.0034]}{1.6696\ [0.0034]}, \quad (8b)$$

$$\mu_s'(\lambda_0) = \frac{R_{m-100}(\lambda_0) + 1.5437\ \left[-0.0126\ R_{m-100}(\lambda_0)^2 + 0.0074\, R_{m-100}(\lambda_0) + 0.0027\right]}{1.6696\ \left[-0.0126\ R_{m-100}(\lambda_0)^2 + 0.0074\, R_{m-100}(\lambda_0) + 0.0027\right]}, \quad (8c)$$

where Eqs. (8b) and (8c) are for the constant $a_{0\text{-}100}$ and quadratic $a_{0\text{-}100}$, respectively.

4. Methodology

4.1 Instrumentation

The experimental set-up for R_m measurements consisted of a tungsten-halogen light source (LS-1, Ocean Optics, Inc., Dunedin, FL), bifurcated fiber optic probe, data acquisition card (DAQ-700), spectrometer (SD2000, Ocean Optics, Inc., Dunedin, FL) with wavelength grating from 350-950 nm and a laptop computer [2, 11]. The fiber optic probe contained two 400-μm (or 100-μm) diameter fibers for light delivery and light collection, respectively, with an outer diameter of 1.3 mm (or 0.4 mm). The center-to-center distance between the source and detector fibers was approximately 400 μm (or 100 μm) for the 400-μm (or 100-μm) probe. A cross-section drawing for the 400-μm probe is shown in Fig. 3(a). The reflected signal passed through the optical fiber, dispersed and detected by the CCD spectrometer, and the electrical signal for the spectrometer output was sent to the computer [22, 24]. LabView interface software (National Instruments, Austin, TX) was used between the spectrometer and laptop to display the optical reflectance in real-time.

All effects from the fiber, light source and spectrometer have been removed by dividing each optical reflectance signal by a calibration curve taken from a standard reflectance sample [25, 26]. The standard sample surface provides approximately 100% reflectance in the wavelength range of 250-2000 nm (Diffuse Reflectance Standard Specifications, Ocean Optics, FL). The calibration reflectance was obtained by placing the probes on top of the standard sample and recording the reflected signals. Moreover, it is practically important to note that in spite of turning off all room lights and covering the sample container, a small level of background due to thermal noise of the CCD array was still present. By recording

#7239 - $15.00 USD Received 22 April 2005; revised 7 June 2005; accepted 9 June 2005

this background signal prior to the actual measurement and subtracting it from the raw data, we could obtain improved a_0 values.

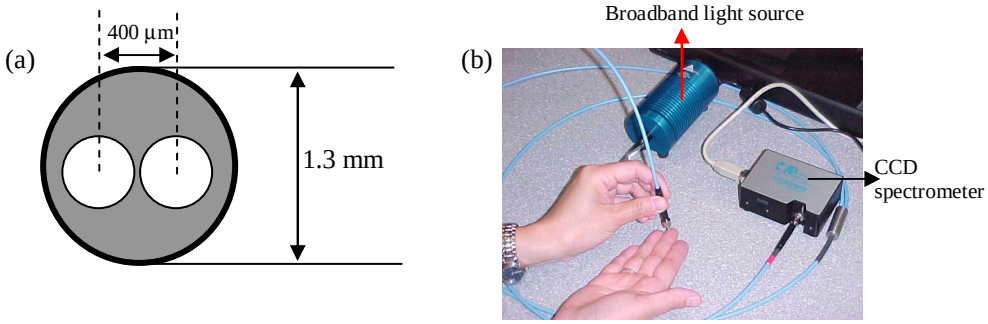

Fig. 3. (a). The schematic cross section of the 400-µm fiber probe. 3(b). Experimental setup for the *in vivo* reflectance measurements of the human middle finger. The particular probe shown above is just for the demonstration purpose and equivalent to the 400-µm probe, which was used for the determination of μ_s' values of human fingers. Also, the broadband light source and CCD spectrometer are shown, as labeled.

The dual-channel ISS oximeter (ISS, Champaign, IL) was the "gold standard" instrument and used to measure the reduced scattering coefficient from each sample solution. More details on the ISS oximeter can be found through ref. [23]. Basically, the device works by emitting NIR light into tissue at known distances from a collector. Light of two different wavelengths is used, and the light is modulated at an RF (radio frequency) of 110 MHz. The collected light is measured and processed, and the absorption and reduced scattering coefficients of the medium are determined. This technology allows the absolute measurement of light absorption and scattering in a highly scattering medium, such as human tissue. In our study, the two channels at 750 nm and 830 nm were used.

To compare the calculated μ_s' values determined from the reflectance probes with the ISS 'gold standard" readings, we used relative error calculations to express the deviation between them as follows:

$$\text{Relative error in } \mu_s' = \frac{\left|\mu_s'(\text{probe}) - \mu_s'(\text{ISS})\right|}{\mu_s'(\text{ISS})} 100\% \qquad (9)$$

4.2 In vitro measurements using Intralipid

In vitro measurements were performed using a diluted solution of Intralipid to simultaneously measure the reduced scattering coefficient and optical reflectance. An Intralipid solution was chosen since it closely simulated light scattering properties of tissue with an estimated g value > 0.9 and a mean particle size of 0.5 µm. A rectangular, plastic container with the volume of 8 cm x 10 cm x 14 cm (height x width x length) was used to hold the testing Intralipid solution. The probes were inserted from the top into the solution during the measurement, so there was no intralipid-container or intralipid-air interfaces for the probe. The probe tip was facing vertically down towards the bottom of the container, a few centimeters below the solution surface, and a few centimeters away from the walls of the container.

All measurements were performed with an integration time of 40 msec for the 400-µm probe, and 100 msec for the 100-µm probe. The Intralipid stock solution was 20% by volume (Pharmacia and Up-John, Clayton, NC), and the diluted Intralipid solutions ranged in concentration from 0.5% - 8%, depending on the optical probe being used. Five spectral readings per location were taken during the Intralipid measurements for the 400-µm probe. In general, the reduced scattering coefficients, μ_s', found in tissues vary between 5 and 25 cm^{-1}; however, larger values of μ_s' have been reported in brain tissues [21, 22]. After the

#7239 - $15.00 USD Received 22 April 2005; revised 7 June 2005; accepted 9 June 2005

reflectance spectra were taken at different Intralipid concentrations, Eqs. (6b) and (6c) were used to calculate μ_s' values at 750 nm and 830 nm, and they were compared with the expected μ_s' values obtained from the ISS system. Similar procedures were used for the 100-μm probe, except that multiple locations (3 times) per Intralipid solution were taken for the measurement to decrease noise due to small source-detector separation (see more details in Section 5).

4.3 In vivo measurements from human fingers

To obtain the μ_s' values of human fingers *in vivo*, the 400-μm probe was placed against the surface of the skin of a human (index or middle) finger with the tip of the probe lightly touching the skin, as shown in Fig. 3(b), without any compression. Uncompressed touch is to keep local hemoglobin oxygen levels unperturbed. The hand was rested on the table comfortably while the bifurcated fiber probe was facing down in contact with the finger to collect the *in vivo* data. The optical reflectance readings took place less than 100 ms.

4.4 In vivo measurements from living rat brain tissues

To obtain the μ_s' values of living animal brain tissues *in vivo*, experiments were performed using male Sprague-Dawley albino rats. The rats were anesthetized using Nembutal and were mounted in a stereotaxic device. Lidocaine was used to locally anesthetize pressure points near the ears and snout that were in contact with the stereotaxic frame. Since the ventilation, perfusion, and blood oxygenation of the animals were normally not alternated much during the optical measurements, those parameters were not monitored. The experiments were performed in accordance with the guidelines for the ethical use of animals established by the Society for Neuroscience. The University of Texas Southwestern Medical School's Institutional Animal Care and Use Committee approved the experiments. Following an incision in the scalp, a drill was used to bore a small hole in the skull. Through this hole passed the 100-μm probe. The NIR probe was advanced from the dorsal surface of the cerebral cortex, down to a depth of 4 to 8 mm in steps of 200 μm. It was expected that the probe would traverse the cortex (CTx), enter the corpus callosum, extend down into the caudate putamen (CPu), and end above the anterior commissure (ac) [11, 22]. The location of gray and white matter was estimated by referring to rat stereotaxic atlas [27].

5. Results

5.1 In vitro – Intralipid data

With different concentrations of Intralipid solutions, we obtained readings of μ_s' and $R_{m\text{-}400}$ using both the ISS oximeter and optical reflectance, respectively (Fig. 4). Both μ_s' and $R_{m\text{-}400}$ are linearly proportional to Intralipid concentration (%) with a correlation coefficient of 0.971 and 0.995, respectively. Each data point was obtained by averaging the data (750 and 830 nm) from five different measurements at each concentration. A similar graph was also obtained (data not shown) for the 100-μm probe.

Figure 4 shows the μ_s' values, as labeled through the vertical right axis, that were obtained directly from the ISS oximeter readings. The vertical left axis shows the values of $R_{m\text{-}400}$, which can be converted to μ_s' (cal) using Eqs. (6b) and (6c). We employed Eq. (9) to quantify the errors of μ_s' that were calculated using the reflectance readings. Figure 5 presents the error comparison between the expected μ_s' (ISS) and calculated μ_s' (cal) values, using the constant $a_{0\text{-}400}$ (= 0.065 ± 0.01) and the polynomial $a_{0\text{-}400}$, i.e., Eq. (5). This figure demonstrates that the relative errors of calculated μ_s' range up to 35% with a mean ± standard deviation of 16 ± 11%, when the constant $a_{0\text{-}400}$ is used. The relative errors are reduced to less than 10% when using the polynomial $a_{0\text{-}400}$ (mean ± standard deviation: 3.5 ± 3.2%). The range of μ_s' values used for this error analysis is from 5.7 cm^{-1} to 26.7 cm^{-1}, which are the common μ_s' values well known for biological tissues. Thus, this error comparison serves as

#7239 - $15.00 USD Received 22 April 2005; revised 7 June 2005; accepted 9 June 2005

validation and justification for the polynomial $a_{0\text{-}400}$, or Eq. (6c), to be used in the future for μ_s' quantification from a reflectance measurement with the 400-μm probe.

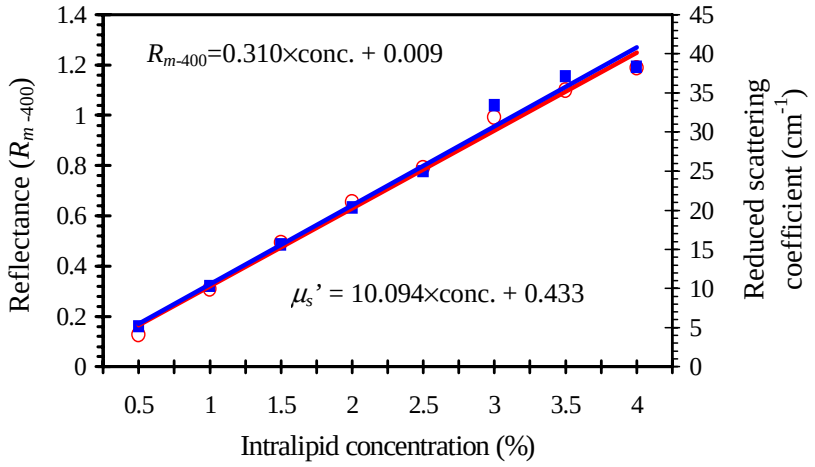

Fig. 4. Linear relationships between 1) the Intralipid concentration and the reflectance (red circles) and 2) the Intralipid concentration and the μ_s' values (blue solid squares) obtained from the ISS oximeter. The data are fitted with linear relationships for the reflectance (red line) and the μ_s' (blue line), respectively, for the 400-μm probe. Specifically, the linear relationships are $R_{m\text{-}400}$ = 0.310×[Intralipid concentration]+0.009 and μ_s'=10.094× [Intralipid concentration] + 0.433 in cm^{-1}.

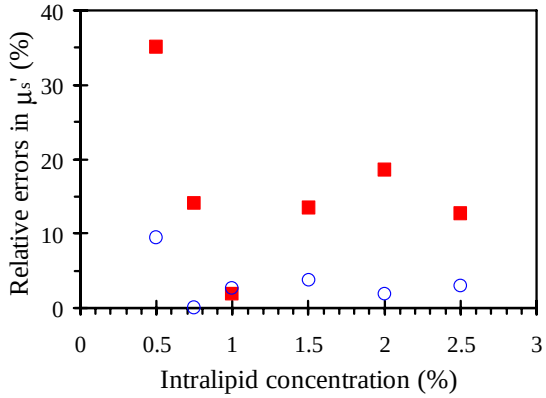

Fig. 5. Error comparison between expected μ_s' (ISS) and calculated μ_s' (cal) values, using the constant $a_{0\text{-}400}$ (= 0.065 ± 0.01) (filled red squares) and the polynomial $a_{0\text{-}400}$, i.e., Eq. (5) (open blue circles). All of the data points were based on five readings per location per Intralipid concentration. The data at 750 nm were used for this comparison.

To investigate the accuracy of ignoring absorption effects, as mentioned in Section 2, we conducted the experiments without and with an ink solution mixed in the Intralipid solution so as to induce light absorption, using the 400-μm probe. The results are shown in Fig. 6, where the μ_a values are 0.04 cm^{-1} and 0.4 cm^{-1} for the two respective cases. Similar to the Monte Carlo results seen in Fig. 1, the reflectance values with the ink solution (i.e., μ_a =0.4 cm^{-1}) are little lower than those without ink. However, the error calculation shows that the relative deviations between the two cases are about or less than 10%. Such an error range supports our approach that when a needle-like probe is utilized, light absorption effect is insignificant and can be reasonably ignored without losing too much accuracy.

#7239 - $15.00 USD
Received 22 April 2005; revised 7 June 2005; accepted 9 June 2005

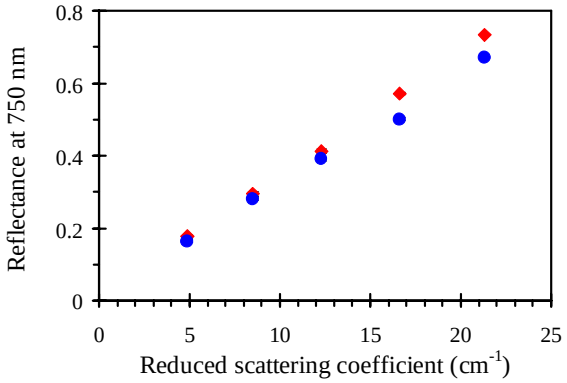

Fig. 6. Linear relationships between the reduced light scattering coefficient (μ_s') and the reflectance measured without ink (red diamonds) and with ink (blue circles). The absorption coefficients of Intralipid solutions without ink and with ink are 0.04 and 0.4 cm^{-1}, respectively. The experiment was taken with the 400-µm probe, and the different values of μ_s' were obtained by varying the Intralipid concentration. The data at 750 nm were used for this comparison.

Additional experiments were performed using the 100-µm probe in order to validate Eqs. (8b) or (8c). In this case, the Intralipid concentrations for the experiment ranged from 1% to 8%. For each Intralipid concentration, three spectra were averaged at each probe location to collect one spectrum, and four measurements were repeated at different random locations within the solution volume for each of the concentrations. Thus, there were 12 spectra collected and averaged for the calculated μ_s'. Then, we performed the comparison between the expected and calculated μ_s' values with the constant $a_{0\text{-}100}$ and polynomial $a_{0\text{-}100}$, i.e., using Eqs. (8b) and (8c). The range of μ_s' values used in this case is from 9.7 cm^{-1} to 76.9 cm^{-1}, covering a broad range of μ_s' values known for biological tissues.

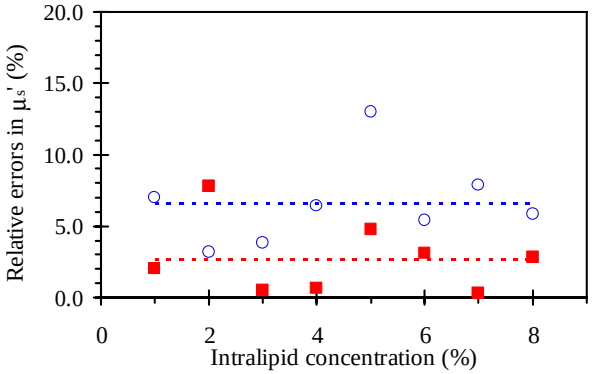

Fig, 7(a). Error comparison between expected μ_s' (ISS) and calculated μ_s' (cal) values, using the constant $a_{0\text{-}100}$ (= 0.0034 ± 0.0005) (shown as filled red squares) and the polynomial $a_{0\text{-}100}$, i.e., equation (7) (shown as open blue circles). The horizontal dashed lines are the mean values of the open-circle and filled-square data points, respectively. To decrease noise due to small a source-detector separation, 4 locations per Intralipid solution were taken for the measurement, and 3 readings per location were used. The data at 750 nm were used for this comparison.

The data given in Fig. 7(a) illustrate that the relative errors of calculated μ_s' vary below 10% (mean ± standard deviation: 2.7 ± 2.6 %) when the constant $a_{0\text{-}100}$ is applied, whereas the relative errors increase above 10% (mean ± standard deviation: 6.6 ± 3.0 %) when using the

#7239 - $15.00 USD
Received 22 April 2005; revised 7 June 2005; accepted 9 June 2005

polynomial $a_{0\text{-}100}$. It is clearly shown that the deviation with the polynomial $a_{0\text{-}100}$ was more than that with the constant $a_{0\text{-}100}$. This analysis suggests that the constant $a_{0\text{-}100}$, or Eq. (8b), is the suitable approach to use for μ_s' quantification with the 100-μm probe in the future.

To further demonstrate the necessity of multiple readings for the 100-μm probe [28], additional comparison was plotted to examine the developed algorithms, Eqs. (8b) and (8c). The experimental results shown in Fig. 7(a) are replotted in Fig. 7(b) together along the data taken with a single reading at a single location. Figure 7(b) clearly reveals that when $R_{m\text{-}100}$ were calculated using data taken at multiple locations with an average of three spectra per location, the relative errors have been greatly reduced in comparison to that obtained with a single measurement at a single location. This conclusion holds for either the constant $a_{0\text{-}100}$ or polynomial $a_{0\text{-}100}$.

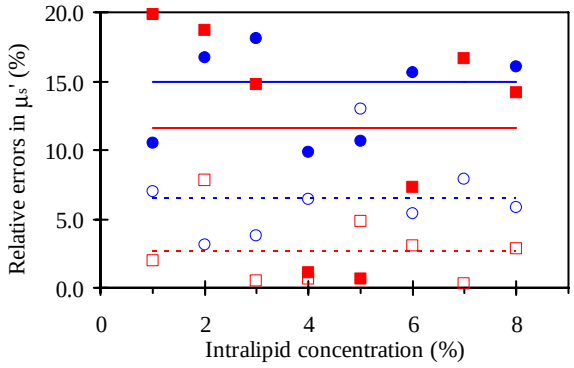

Fig. 7. (b). Error comparison in μ_s' when using a single location measurement (constant $a_{0\text{-}100}$: filled red squares with the mean value plotted by solid red line; polynomial $a_{0\text{-}100}$: filled blue circles with the mean value by solid blue line) versus the average of three measurements per location (constant $a_{0\text{-}100}$: open red squares with the mean value by dashed red line; polynomial $a_{0\text{-}100}$: open blue circles with the mean value by dashed blue line). The data at 750 nm were used for this comparison.

In Section 5.1, we have experimentally tested and validated the newly developed algorithms for both the 400-μm and 100-μm probes, which can be now utilized to derive μ_s' values of tissues *in vivo*. In Sections 5.2 and 5.3 next, we will provide examples to employ the new algorithms for quantification of tissue μ_s' values.

5.2 In vivo – human data

The calculated μ_s' values of the human finger tissues under the uncompressed state, using Eq. (6c), were averaged over 5 measurements at different but adjacent locations from each of 3 human subjects with the 400-μm probe. The μ_s' values at 750 nm are 8.6 ± 2.0 cm^{-1} (mean ± standard deviation), being consistent well with those of *in vivo* human breast tissue at 750 nm reported by Cerussi *et al*. (8.8 cm^{-1}) and Durduran *et al*. (8.3 ± 2.0 cm^{-1}) [29, 30].

5.3 In vivo – rat brain data

Next, we applied Eq. (6c) to the reflectance data measured from the surface of a rat brain to ~6.5 mm deep in the brain, using the 400-μm probe. The NIR probe was advanced from the dorsal surface of the cerebral cortex. Figure 8 shows that the μ_s' values vary between 10 and 35 cm^{-1} at 750 nm, depending upon the particular type of brain tissue being interrogated. According to the corresponding histology, the tissues at the first 1 to 2 mm near the brain surface are gray matter (made of nerve cell bodies and nerve terminals), and the tissue near the peak of μ_s' at ~3.6 mm is located in white matter (made of myelinated and unmyelinated axons) [11]. Indeed, the histology has proven that the probe path traverses the cortex (CTx),

#7239 - $15.00 USD Received 22 April 2005; revised 7 June 2005; accepted 9 June 2005

enters the corpus callosum, extends down into the caudate putamen (CPu), and ends above the anterior commissure (ac) [11, 28].

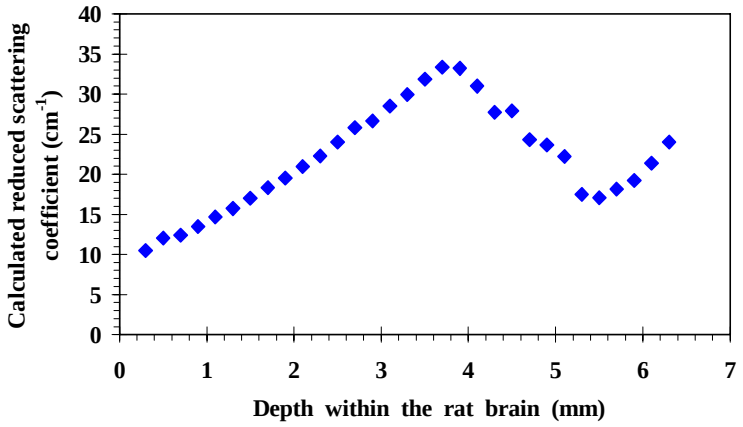

Fig. 8. Calculated reduced scattering coefficients, μ_s', from living rat brain tissues at 750 nm; the data were obtained using the 400-μm probe.

Another measurement and calculation were repeated from a second rat using the 100-μm probe, and the data is shown in Fig. 9. This figure shows clearly that the μ_s' values of the rat brain gradually increase from 15 to 61 cm^{-1} at 750 nm as the probe passes through from gray matter to white matter. Notice that there exists a dip in μ_s' at around 5.4 mm and 4.5 mm in Figs. 8 and 9, respectively. This decrease in μ_s' has proven to result from a piece of intracranial gray matter underlying the white matter [11]. Both of the figures taken from animal experiments *in vivo* strongly illustrate that the μ_s' values of white matter in living animal brains can be quite large, ranging from 35 cm^{-1} to 60 cm^{-1}.

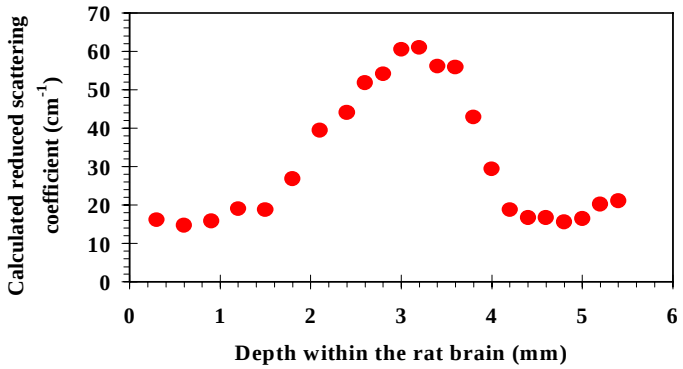

Fig. 9. Calculated μ_s' values from living rat brain tissues at 750 nm; the data were obtained using the 100-μm probe.

6. Discussions and conclusions

By using Monte Carlo simulations and experimental methods, we were able to empirically develop analytical expressions to extract μ_s' values from a single optical reflectance measurement. The key factor in deriving the expressions is to quantify the overall intensity factor, a_0, which depends strongly on the fiber probe geometry. By calibrating a_0 for both the 400-μm and 100-μm probes using the ISS oximeter, we arrived at Eqs. (6) and (8) as the

#7239 - $15.00 USD Received 22 April 2005; revised 7 June 2005; accepted 9 June 2005

appropriate expressions for μ_s' quantification. Such an algorithm allows μ_s' values of various tissues to be measured *in vivo* in real-time, which is useful during surgeries or "optical biopsies" where instant information is important. However, one should be cautious to employ them when the reduced light scattering coefficient becomes significantly low. Errors may occur when μ_s' is near or smaller than 2 cm^{-1}, which is not often seen within biological tissues. It could be possible to re-derive other empirical equations, using either linear (with a zero intercept) or higher order forms.

Several experiments with different concentrations of Intralipid were performed to gather additional data in order to validate the algorithms. The data at 750 nm were used to determine if there was a difference in μ_s' calculations using a constant a_0 versus a polynomial a_0 for both of the probes. Statistical analysis showed that the polynomial $a_{0\text{-}400}$ produced improved μ_s' values for the 400-μm probe, while the constant $a_{0\text{-}100}$ produced improved μ_s' for the 100-μm probe.

In the calibration study, we learned that the μ_s' data obtained at 750 nm and 830 nm can be pooled together to generate Eqs. (6) and (8). Given the fact that light scattering of biological tissues in the NIR range does not strongly depend on wavelength [3, 4], we suggest that Eqs. (6) and (8) can be approximately valid in the wavelength range of 700 nm to 850 nm without causing significant errors.

Why can relatively simple algorithms, such as Eqs. (6) and (8), be developed to determine μ_s' using reflectance data? Our answer is that the absorption coefficient, μ_a, of the tissue has much less contribution to light reflectance when the light source and detector are nearby, in a few hundred microns. The Monte Carlo simulations (Fig. 1) and our experimental data (Fig. 6) clearly demonstrate that the reflectance readings did not depend on μ_a strongly when μ_a values ranged from 0.01 cm^{-1} to 0.4 cm^{-1}(0.5 cm^{-1}), which are the typical μ_a values seen in biological tissues. In the NIR region, μ_a is normally much smaller than μ_s', and thus the absorption length (=1/μ_a) is much longer than the reduced scattering length (1/μ_s'). In the case of needle-like probes with a source-detector separation of a few hundred microns, the absorption length is much larger than the separation so that the effect of μ_a can be reasonably ignored without causing a significant error. Thus, the algorithms developed in this study have the theoretical foundation and can be applicable only in the NIR range.

It is noted that the data taken with the 100-μm probe are noisier than those with the 400-μm probe [28]. We hypothesize that the noisy feature is possibly attributed to the dimension of source-detector separation of the 100-μm probe. In many cases of Intralipid measurements, the separation was comparable to the single scattering length of the Intralipid solution, so the statistical noise became severe. Namely, we suggest that Brownian motion of the lipid particles during the time course of a measurement may contribute to the higher noise in the data obtained with the 100-μm probe. Thus, it is more important to average several measurements within the sample solution when the 100-μm probe is used. We expect that this kind of noise should decrease in solid tissues because of limited random motion of scatterers. Indeed, we observed much less deviation in measurements of biological tissues during the course of our human and animal studies [11, 12, 22]. Further experimental confirmation for this hypothesis can be performed by lowering the temperature of the solutions or adding an agent that would increase its viscosity.

The calculated μ_s' values from the living rat brain tissues ranged from 10-61 cm^{-1} in our measurement. As mentioned in Section 5, the rat brain data reveal that the μ_s' values of white matter are relatively high, ranging 35-60 cm^{-1} in the two animal brains reported in this paper. We have consistently observed similar μ_s' values of white matter in other animal experiments (more than 8 rat brains) [22]. Indeed, to the authors' knowledge, this is the first report to provide the μ_s' values of living white matter *in vivo*, and the first study to show good consistency between the μ_s' values taken *in vivo* in our study and those measured *in vitro*, as reported by other groups [21, 31, 32].

#7239 - $15.00 USD Received 22 April 2005; revised 7 June 2005; accepted 9 June 2005

The results obtained from living rat brain tissue (using both probes) are consistent with those published by Cheong *et al*. [20], where the reduced scattering coefficients were reported to vary from 6.6 cm^{-1} in a calf brain at 633 nm to 57 cm^{-1} in a pig brain at 633 nm. It is highly possible that the low μ_s' value resulted from a piece of gray matter, and the high μ_s' value came from a piece of white matter. Furthermore, it is important to note that the published results were obtained all from post-mortem tissues, whereas our measured data are all from *in vivo* living animal brains.

Shangguan *et al*. conducted experiments to investigate changes in optical properties of elastin lamina, from porcine aorta, as a function of pressure [33]. Their work showed that the μ_s' value increased from 53.7 to 83.1 cm^{-1} (by 57%) when pressure (1 kg/cm^2) was applied to the tissue. Even though this work was conducted on *ex vivo* tissue, it indicates that as tissue is compressed, the reduced scattering coefficient increases. Since the fiber probe applies a force to the brain tissue as it advances through the rat brain, the pressure might cause an increase in μ_s' within a certain degree. However, since the pressure applied at the probe tip should be much less than 1 kg/cm^2, we do not expect a large increase in μ_s' caused by pressure.

The potential utility of μ_s' measurement of tissues is to study the origin of light scattering, leading to the determination of cellular or sub-cellular structures at the local measurement site [3,5]. This is the direction of our future study. Such morphological information, made available in the operating room, may assist the identification of important targets for brain surgery.

In summary, this paper shows that an algorithm can be empirically developed to directly calculate the reduced scattering coefficient from a single optical reflectance spectrum. However, it is important to note that the a_0 term is fiber dependent. Individual calibration procedures and experiments are needed to obtain the a_0 term for individual fiber optic probes, which contain fibers with different sizes and/or different configurations. This study demonstrates a feasible methodology to use a needle-like probe to quantify μ_s' values of various living tissues *in vivo* in real time, which may be practically useful for a variety of biomedical applications.

Acknowledgments

This work was supported in part by the National Institutes of Health 1-R01-NS40874-01 and 1-R21-CA101098-01. The authors are also grateful to Mr. Ali N. Bahadur for his assistance of collecting certain Intralipid data.